Temperature, carbon dioxide and methane

Clive Hambler (1)*, Peter A. Henderson (1,2)

(1) Department of Zoology, University of Oxford, UK, ORCID 0000-0002-2361-828X (2) PISCES Conservation Ltd, UK, ORCID 0000-0002-7461-1758 * corresponding author clive.hambler@zoo.ox.ac.uk

Abstract

1) Globally-representative monthly rates of change of atmospheric carbon dioxide and methane are compared with global rates of change of sea ice and with Arctic and Antarctic air temperatures. 2) Carbon dioxide is very strongly correlated with sea ice dynamics, with the carbon dioxide rate at Mauna Loa lagging sea ice extent rate by 7 months. 3) Methane is very strongly correlated with sea ice dynamics, with the global (and Mauna Loa) methane rate lagging sea ice extent rate by 5 months. 4) Sea ice melt rate peaks in very tight synchrony with temperature in each Hemisphere. 5) The very high synchrony of the two gases is most parsimoniously explained by a common causality acting in both Hemispheres. 6) Results are consistent with a proposed role of a high-latitude temperature-dependent abiotic variable such as sea ice in the annual cycles of carbon dioxide and methane. 7) If sea ice does not drive the net flux of these gases, it is a highly precise proxy for whatever does. 8) Potential mechanisms should be investigated urgently.

Keywords Climate change • Degassing • Outgassing • Productivity • Proxy • Sea ice

Introduction

The seasonal cycles of carbon dioxide and methane are both very strongly correlated with the seasonal cycle of sea ice, suggesting sea ice has a dominant causal role in the cycle or is extremely strongly correlated with whatever does (Hambler & Henderson, 2020a, b). Temperature drives ice melt and should thus be very highly correlated with the monthly rate of change of these greenhouse gasses - whether or not sea ice is involved in the cycles. We test this prediction here.

Temperature is conventionally believed to drive the annual cycles of methane and carbon dioxide through changes in vegetation and microbial productivity, including agriculture (IPCC 2013). However, there is substantial uncertainty in the locations and magnitudes of sources and sinks for these gases (Resplandy et al 2018; Winkler et al 2019) with polar regions being amongst the most poorly known due to challenging logistics (Vancoppenolle & Tedesco 2017; Geilfus et al 2018; Bushinsky et al 2019; MOSAiC 2019). Terrestrial productivity in the Northern Hemisphere, typically measured by NDVI (*e.g.* Keeling et al 2001; Buermann et al 2007), is less strongly correlated with carbon dioxide rates than are sea ice rates (Hambler & Henderson 2020a) and to our knowledge no region has been shown to have extremely high temporal synchrony and hence statistical correlation with the global carbon dioxide rate.

Given the relatively strong correlations we have found with sea ice, we predict very strong synchrony between polar air temperatures and the high latitude fluxes of methane and carbon dioxide (driven mainly by the annual cycle of solar elevation). We hypothesize high-latitude air temperatures drive sea ice dynamics and snow dynamics and thence might influence greenhouse gas dynamics. Such strong relationships are not presented in the review of the carbon cycle that informs international climate policy (IPCC 2013) and could focus greater attention on high latitude sites and fluxes.

Methods

We use the datasets in Table 1.

Table 1 Data sources

Variable	Data source
Atmospheric CO_2 Mauna Loa, Alert and South Pole Monthly flask	NOAA GML Carbon Cycle Cooperative Global Air Sampling Network, 1983-2019, Version: 2020-07-24 https://www.esrl.noaa.gov/gmd/dv/data/ ftp://aftp.cmdl.noaa.gov/data/trace_gases/co2/flask Accessed 1 August 2020 Dlugokencky et al (2020a)
Atmospheric CH_4 Mauna Loa, Alert, Cape Grim and South Pole Monthly flask	NOAA GML Carbon Cycle Cooperative Global Air Sampling Network, 1983-2019, Version: 2020-07-24 https://www.esrl.noaa.gov/gmd/dv/data/ ftp://aftp.cmdl.noaa.gov/data/trace_gases/ch4/flask Accessed 1 August 2020 Dlugokencky et al (2020b)
Atmospheric CH_4 Globally-averaged monthly data	https://esrl.noaa.gov/gmd/ccgg/trends_ch4/ Accessed 1 January 2021 Dlugokencky (2021)
Sea ice extent Monthly mean	https://nsidc.org/data/seaice_index/archives Sea Ice Index Version 3 ftp://sidads.colorado.edu/DATASETS/NOAA/G02135/ (Fetterer et al 2017) 'North' (= 'Arctic'): ftp://sidads.colorado.edu//DATASETS/NOAA/G02135/north/monthly/data/ at sidads.colorado.edu 'South' (= 'Antarctic'): ftp://sidads.colorado.edu/DATASETS/NOAA/G02135/south/monthly/data/ Files in form: S_01_extent_v3.0.csv Accessed 26 February 2020
Snow extent Northern Hemisphere Monthly mean	https://climate.rutgers.edu/snowcover/docs.php?target=datareq NH SCE CDR v01r01 https://climate.rutgers.edu/snowcover/files/moncov.namgnld.txt https://climate.rutgers.edu/snowcover/files/moncov.nam.txt Accessed 27 March 2020
Alert air temperature Monthly mean	NCEP Reanalysis Dataset Produced at NOAA Physical Sciences laboratory https://psl.noaa.gov/data/timeseries/arctic/ Accessed 6 January 2021
South Pole air temperature (Amundsen-Scott South Pole Station) Monthly mean	Amundsen_Scott temperature https://legacy.bas.ac.uk/met/READER/surface/Amundsen_Scott.All.temperature.txt British Antarctic Survey. UK Antarctic Surface Meteorology; 1947 - 2013 http://dx.doi.org/10.5285/569d53fb-9b90-47a6-b3ca-26306e696706 Accessed 16 December 2020

We examine atmospheric gas levels for a site considered globally representative for carbon dioxide (Mauna Loa, Hawaii, USA) (IPCC 2013), and a global average estimate of monthly methane (Dlugokencky 2021). We also examine methane rates at Mauna Loa since these are measurements from what might also be a representative site for methane.

Within the NOAA Global Monitoring Laboratory network of atmospheric gas recording sites we examine the most northerly site (Alert, Canada) and the most southerly (South Pole) since these would be predicted to respond strongly to any temperature-dependent forcing. Having examined all sites in this network with monthly flask data we selected Cape Grim (Tasmania, Australia, latitude 41ºS) as an illustration of the high similarity of phenology of the South Pole to some sites at lower latitudes.

Temperature data (average monthly values in degrees Centigrade) were obtained for meteorological stations at the South Pole and Alert as examples of very high-latitude sites where local gas levels are also monitored. The Alert data were rescaled by subtracting 100, to make all values negative. Temperature values were inverted to visually compare synchrony of peak temperature with peak negative net fluxes of the gases, since we have previously established peak negative flux is tightly synchronous with sea ice melt at high latitudes (Hambler & Henderson 2020a, b).

Methodological consistency is essential in time series analysis (Henderson, 2021) so we use datasets which are very likely to have been quality controlled for methodological drift. A monthly database of sea ice extent is easily available from NSIDC from January 2006, which we therefore use as the start date. Arctic and Antarctic extents were used to calculate the rate for the 'global' sea ice extent (which we term 'Arctic plus Antarctic' rate as in Hambler & Henderson 2020a, b).

Rates of change for variables were derived as follows: rate in month 2 is the mean value in month 2 minus the mean value in month 1.

Statistical analysis was based on the R platform. Cross correlations and consideration of autocorrelation were performed as in Hambler & Henderson (2020b). To examine lags of up to ± 12 months between time series we used the sample cross-correlation function ccf. We used the rcorr function in the Hmisc package to find the significance of the correlation at the lag giving the highest cross correlation.

Due to data availability and other constraints at the time of this work, some time series have different end dates or missing values so are not fully comparable and not all are analysed statistically. Statistical analyses are only performed here for the global levels of methane and carbon dioxide and for one other time series for illustrative purposes (showing a tight visual fit is also supported statistically). The results of any analysis are given in the Figure captions. Previous work (Hambler & Henderson 2020a, b and unpublished) has established that close visual fits using the minima in such time series always have high statistical correlations and often identify the lag between them; this can be confirmed if the work is replicated.

Results

a) Globally representative atmospheric gas measurements

The monthly time series for carbon dioxide rate from Mauna Loa, global sea ice extent rate and an Arctic temperature (Alert, Canada) are given in Fig. 1 and Fig. 2.

Fig. 1 Global monthly carbon dioxide rate (measured at Mauna Loa, lagged 7 months) *vs.* global sea ice extent rate. $r = 0.79$ at lag = 7 months; $p < 0.001$

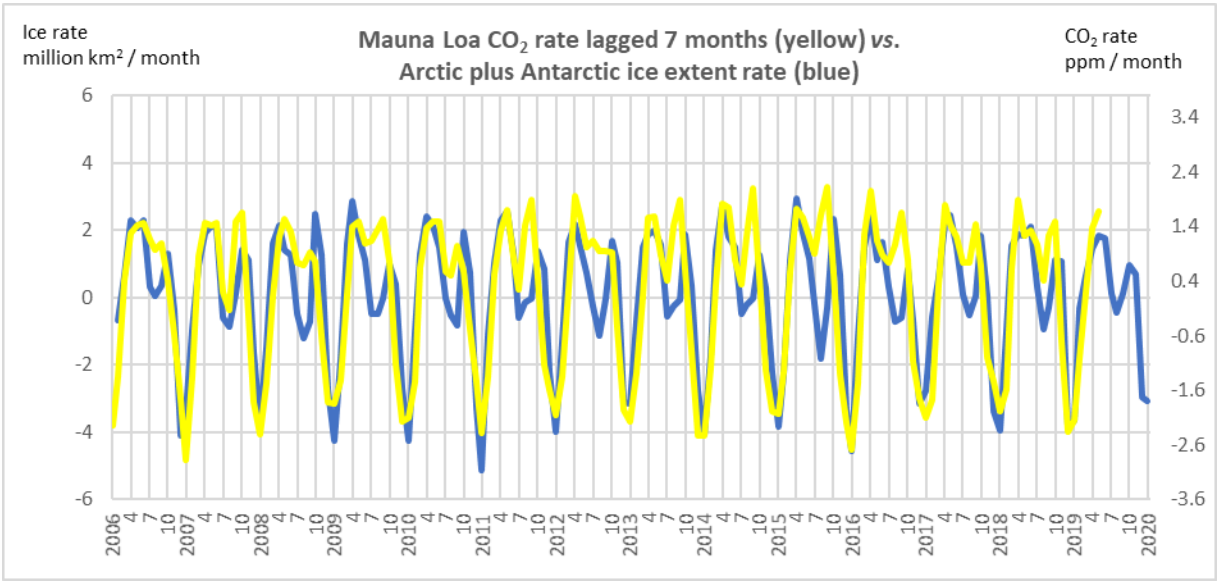

Fig. 2a Monthly carbon dioxide rate Mauna Loa (lagged 1 month) *vs.* temperature at Alert (inverted)

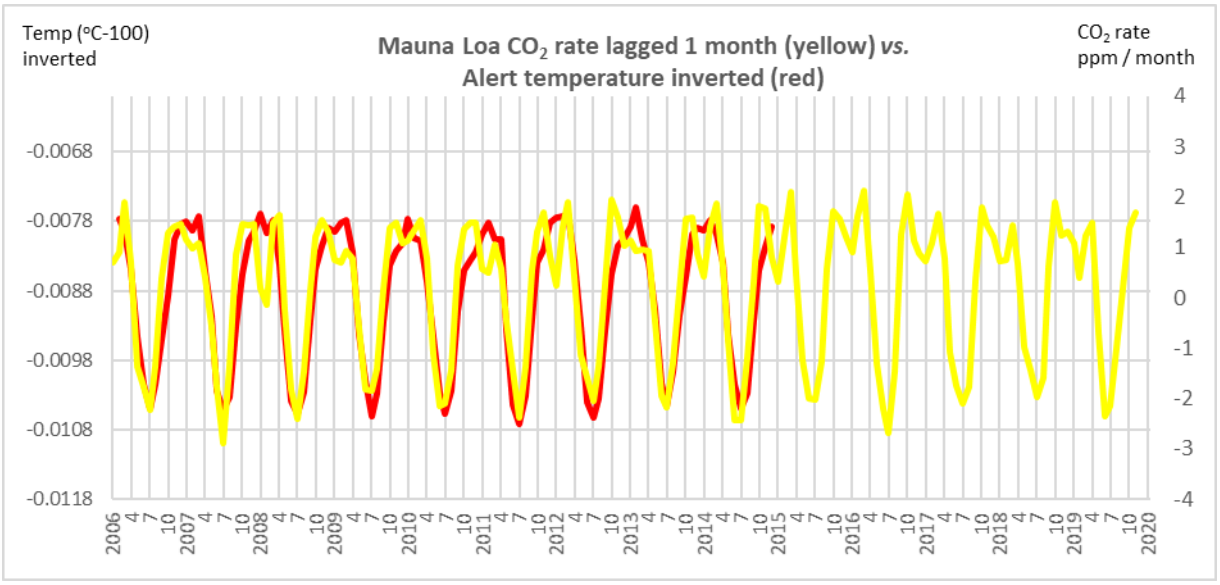

Fig. 2b Monthly carbon dioxide rate Mauna Loa (lagged 1 months) *vs*. temperature at Alert, Canada (inverted), 6 month moving average for both variables

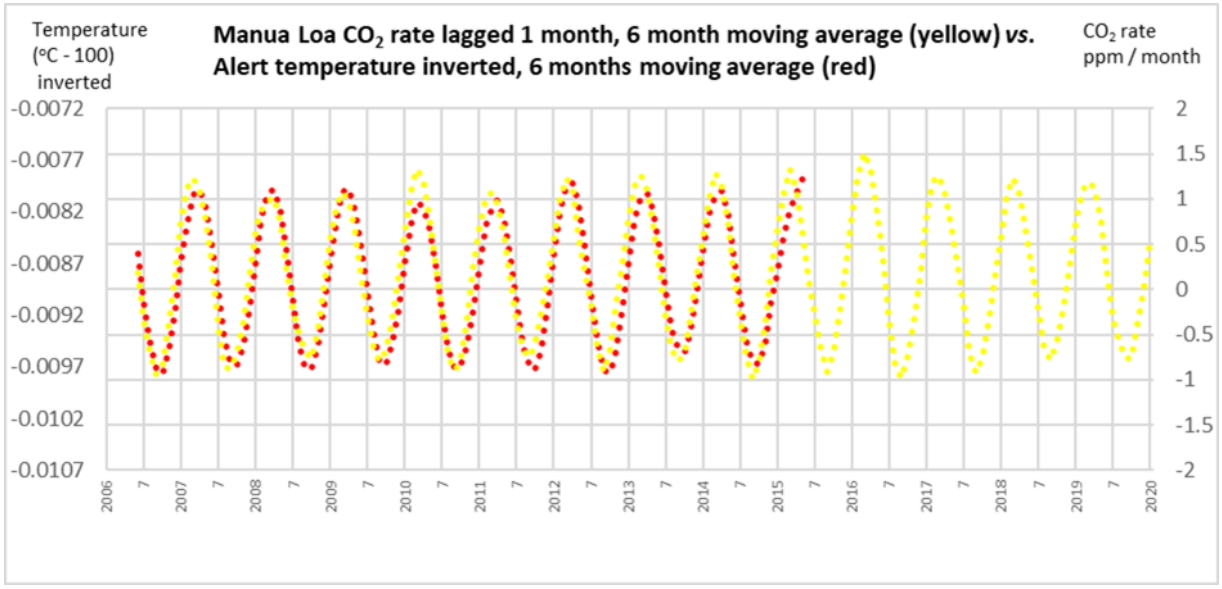

Fig. 2c Monthly carbon dioxide rate Mauna Loa (lagged 1 month) *vs*. temperature at Alert, Canada (inverted), using full continuous monthly Mauna Loa CO_2 record from July 1976

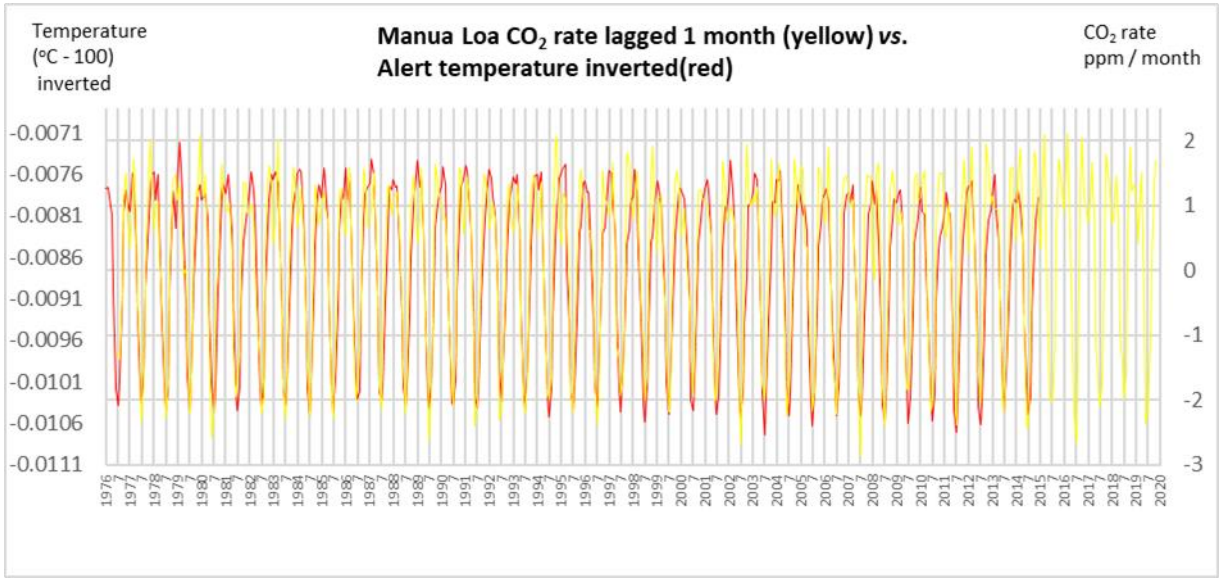

Fig. 2d Monthly carbon dioxide rate Mauna Loa (lagged 1 month) *vs.* temperature at Alert, Canada (inverted), 6 month moving average for both variables, using full continuous monthly Mauna Loa CO2 record from July 1976

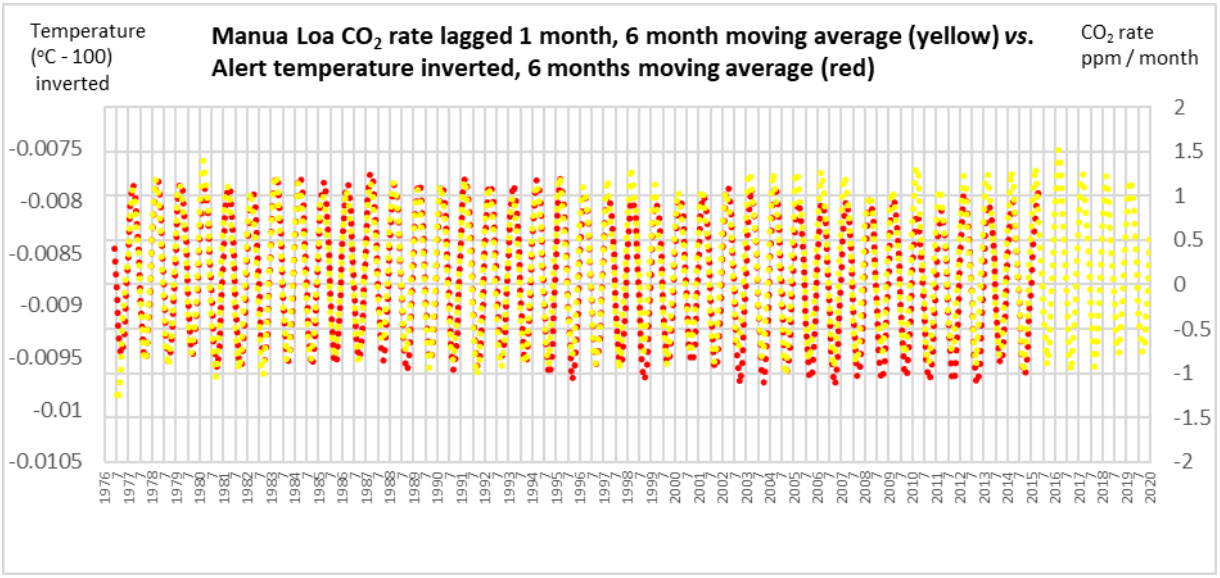

The monthly time series for carbon dioxide rate from Mauna Loa and an Antarctic temperature (South Pole) are given in Fig. 3.

Fig. 3a Monthly carbon dioxide rate Mauna Loa (lagged 7 months) *vs.* temperature at South Pole (inverted)

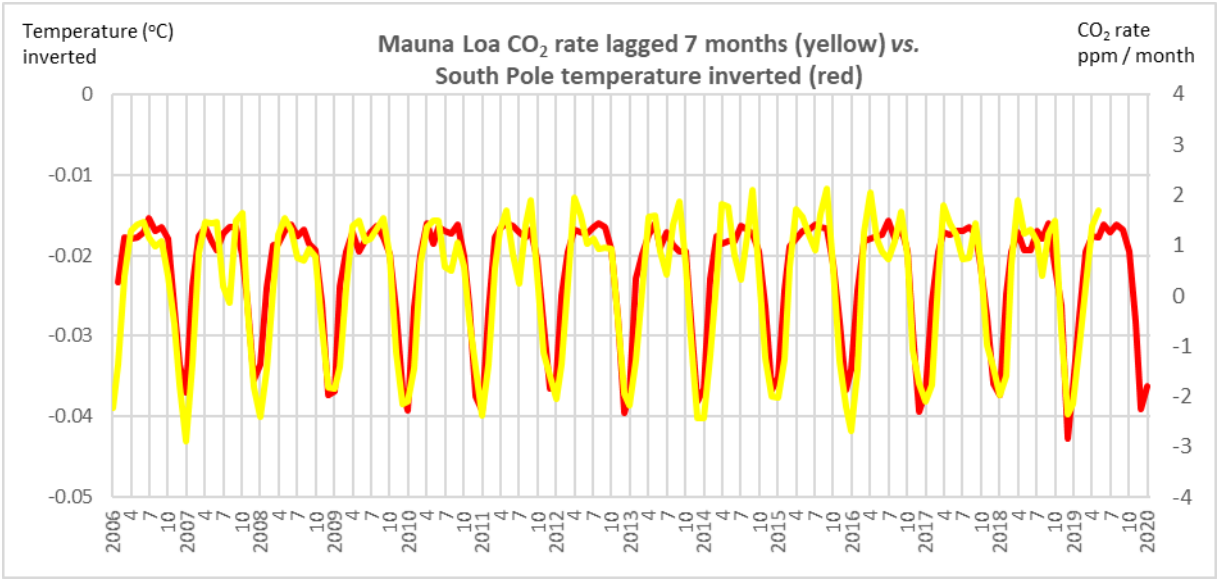

Fig. 3b Monthly carbon dioxide rate Mauna Loa (lagged 7 months) *vs*. temperature at South Pole (inverted), 6 month moving average for both variables

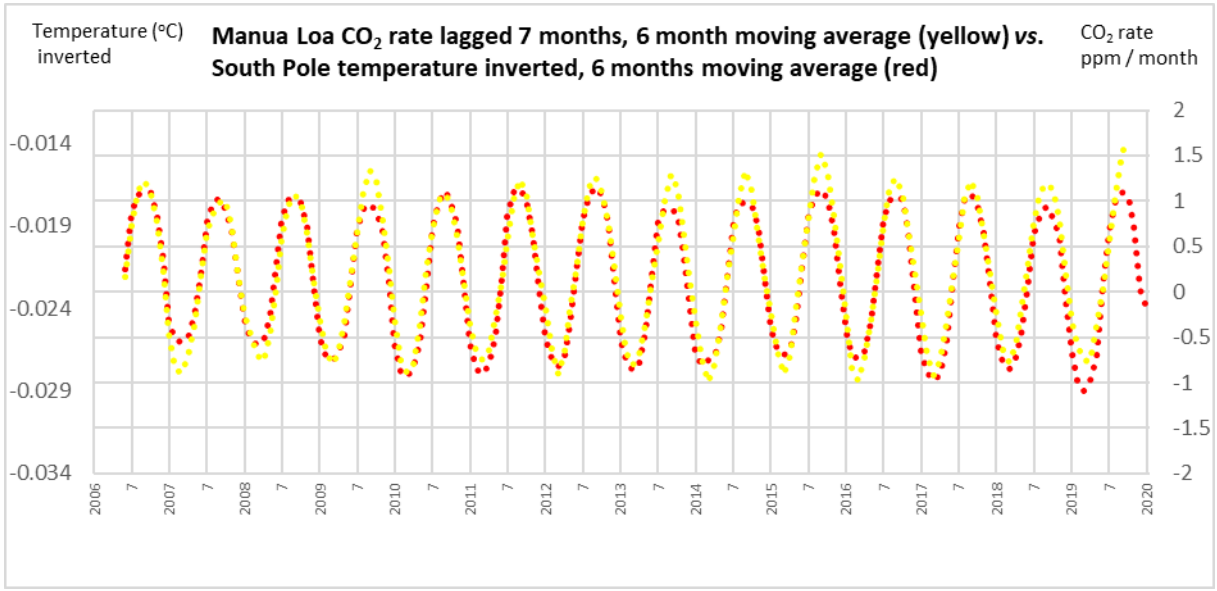

Fig. 3c Monthly carbon dioxide rate Mauna Loa (lagged 7 months) *vs.* temperature at South Pole (inverted), using full continuous monthly Mauna Loa CO_2 record from July 1976

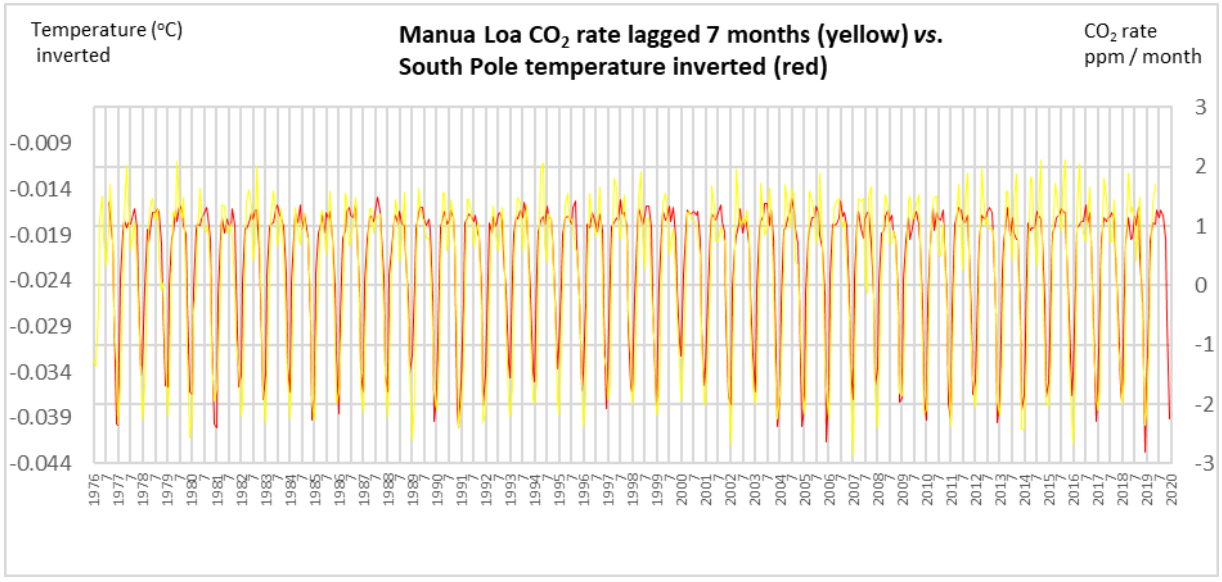

The monthly time series for methane rates averaged from a global network of sites, and from Mauna Loa, are plotted against global sea ice extent rate in Fig. 4 and Fig. 5.

Fig. 4 Monthly global average methane rate (lagged 5 months) *vs.* global sea ice extent rate. $r = 0.78$ at lag = 5 months; $p < 0.001$

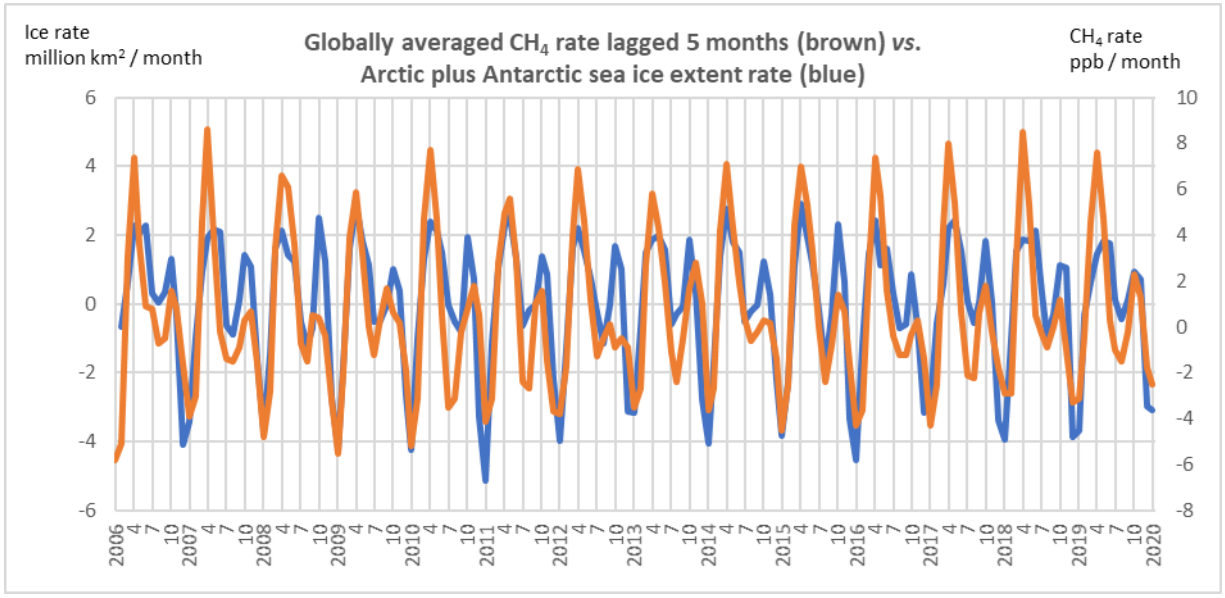

Fig. 5 Monthly methane rate Mauna Loa (lagged 5 months) *vs.* global sea ice extent rate

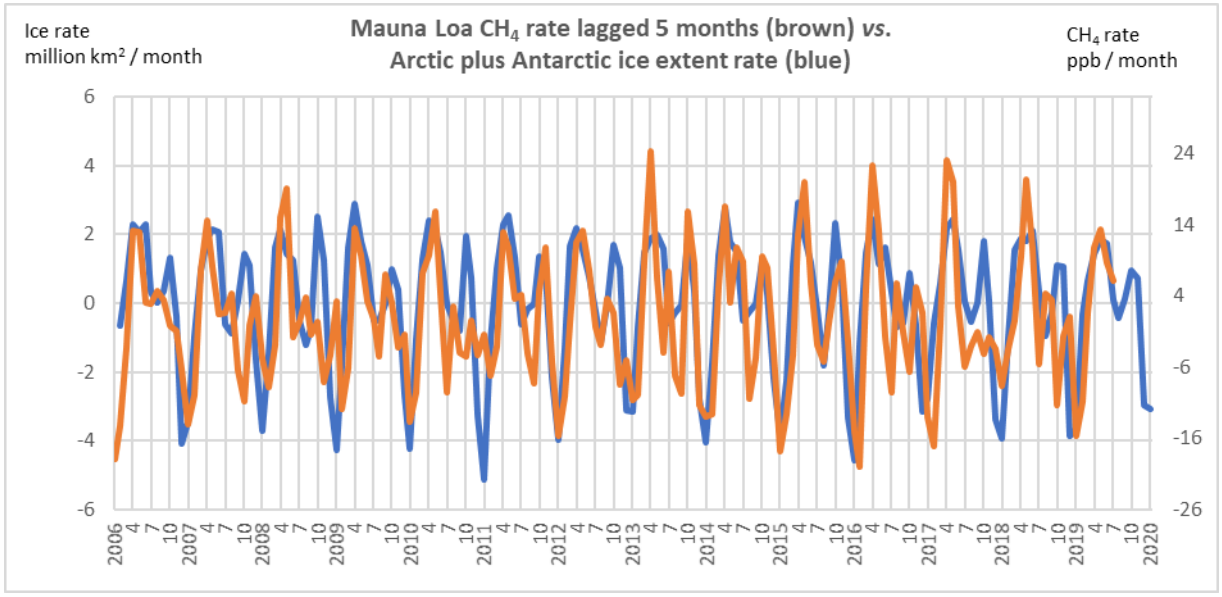

Globally representative carbon dioxide and methane rates are compared in Fig. 6.

Fig. 6 Global carbon dioxide rate (Mauna Loa, lagged 2 months) *vs.* global methane rate

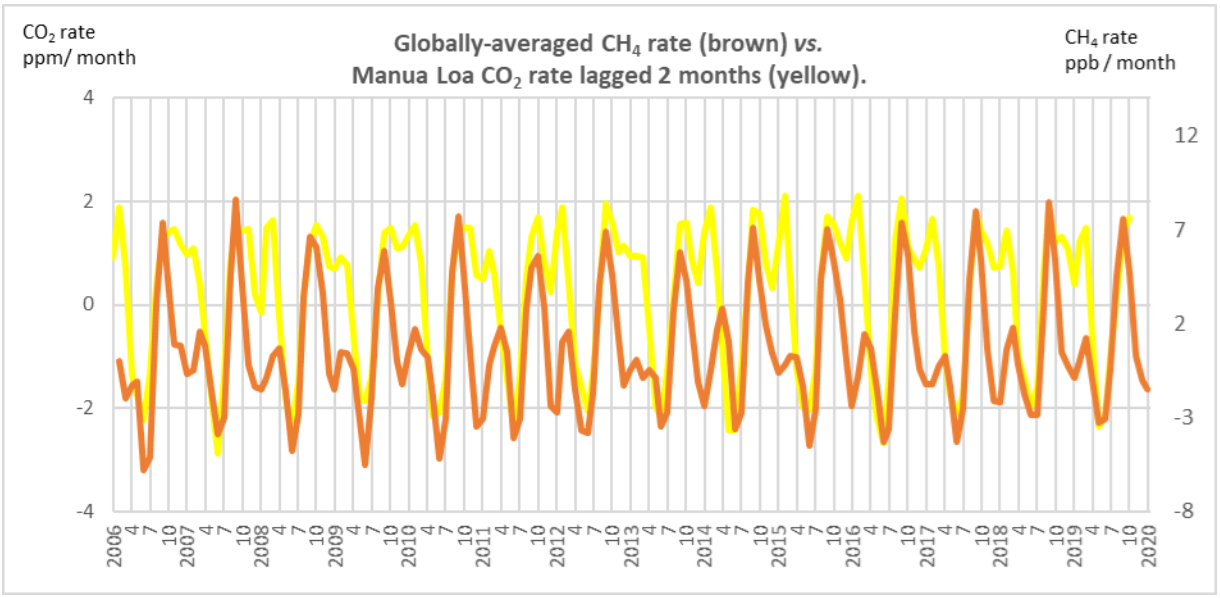

b) Arctic. Monthly time series for carbon dioxide and methane rates at Alert (Canada) plotted against Alert temperature and Northern Hemisphere snow extent rate, are given in Figs. 7 - 9.

Fig. 7 Monthly carbon dioxide rate Alert *vs.* temperature at Alert (inverted)

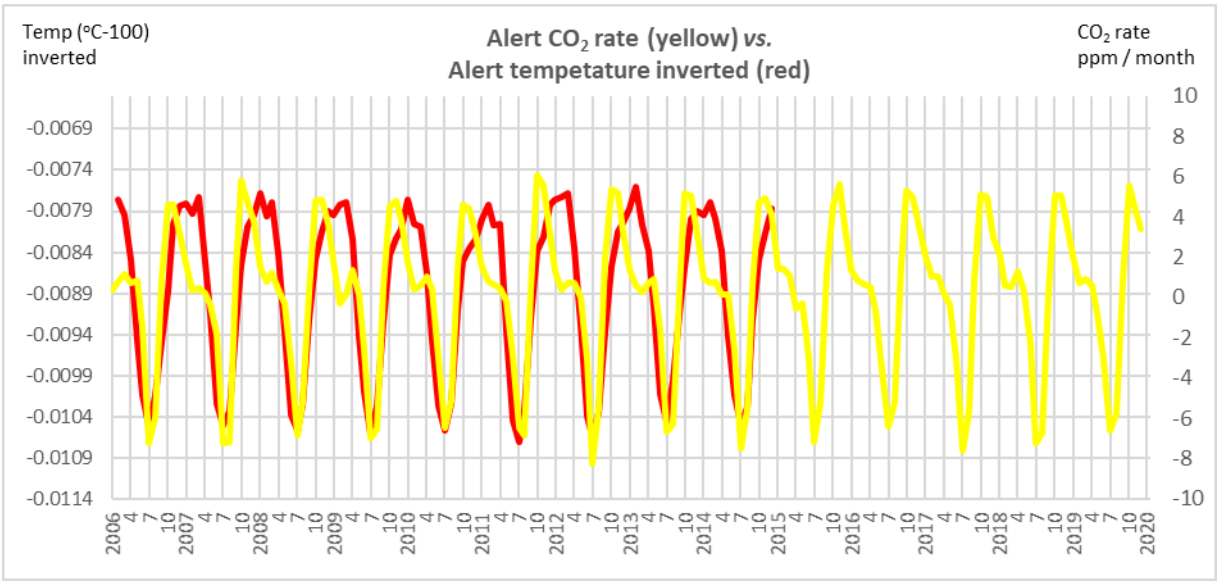

Fig. 8 Monthly methane rate Alert *vs.* temperature at Alert (inverted)

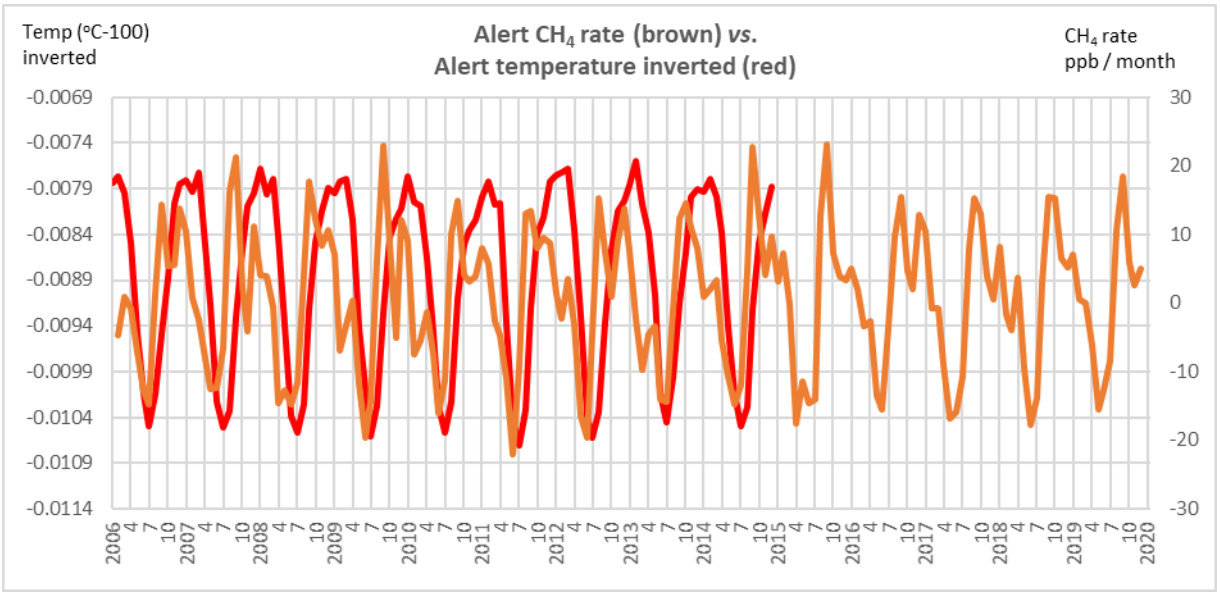

Fig. 9 Monthly methane rate Alert *vs.* Northern Hemisphere snow extent rate

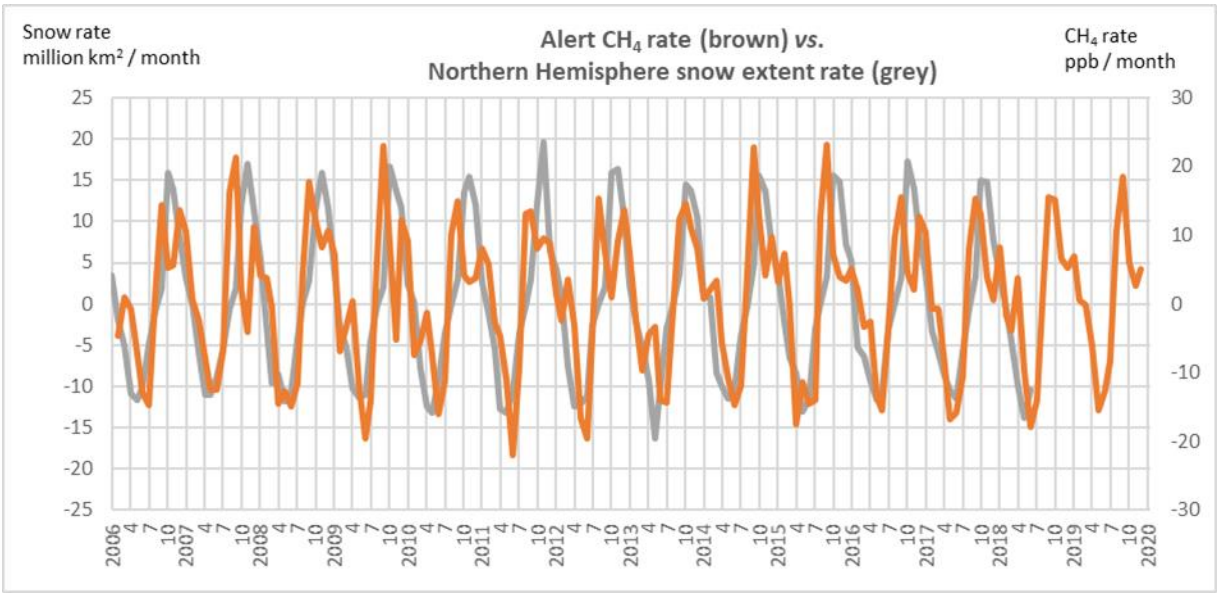

Time series for Arctic sea ice extent rate and a local temperature (Alert) are given in Fig. 10

Fig. 10 Monthly Arctic sea ice extent rate *vs.* temperature at Alert (inverted)

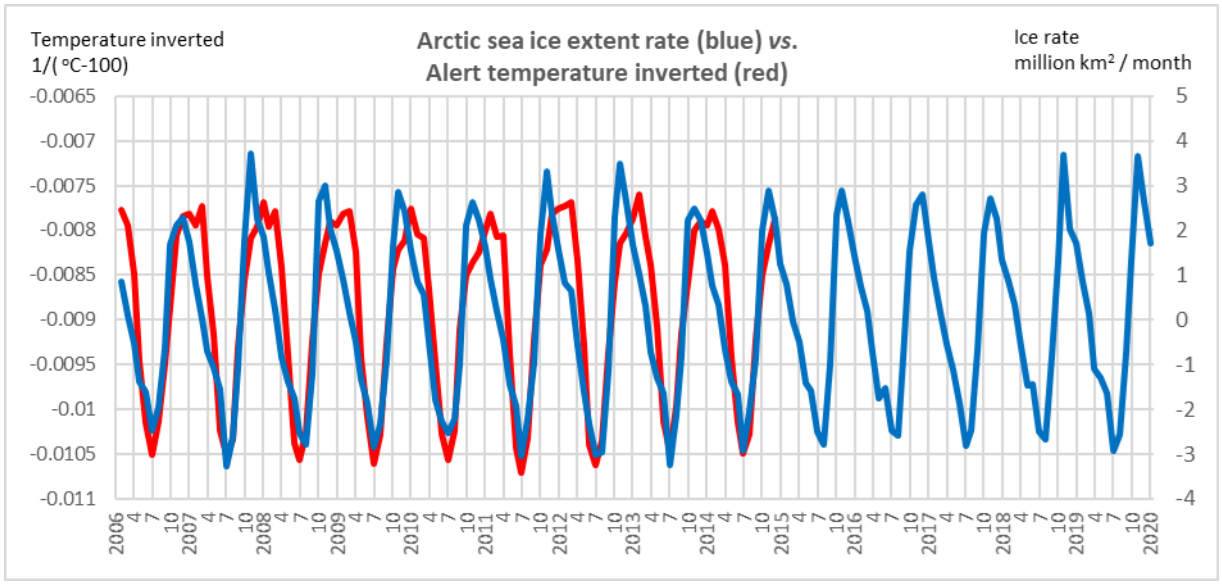

c) Antarctic

Monthly time series of carbon dioxide rate and methane rate at the South Pole, and temperature at the South Pole, are given in Figs. 11 - 13.

Fig. 11 Monthly carbon dioxide rate South Pole (lagged 1 month) *vs.* monthly methane rate South Pole

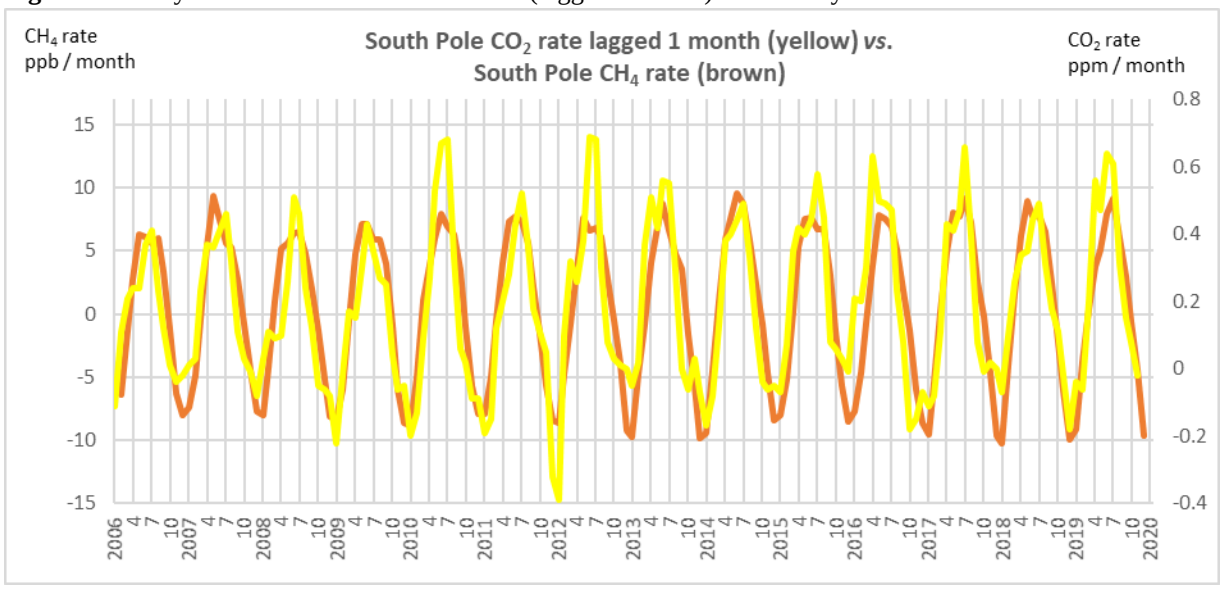

Fig. 12 Monthly carbon dioxide rate South Pole (lagged 1 month) *vs.* temperature at South Pole (inverted)

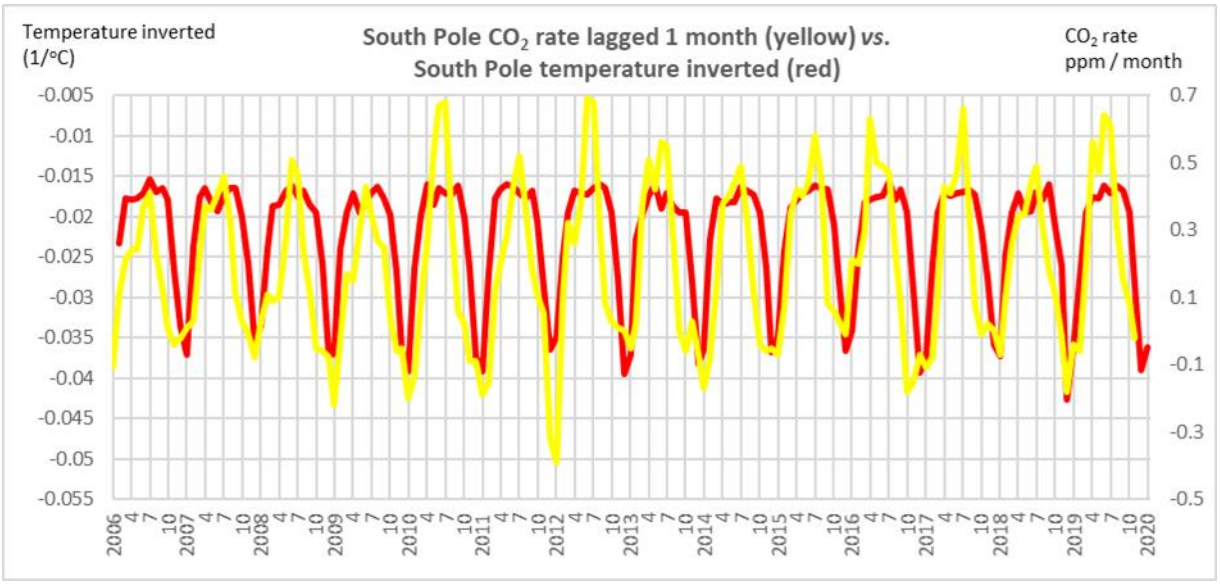

Fig. 13a Monthly methane rate South Pole *vs.* temperature at South Pole (inverted). $r = 0.88$ at zero lag; $p < 0.001$

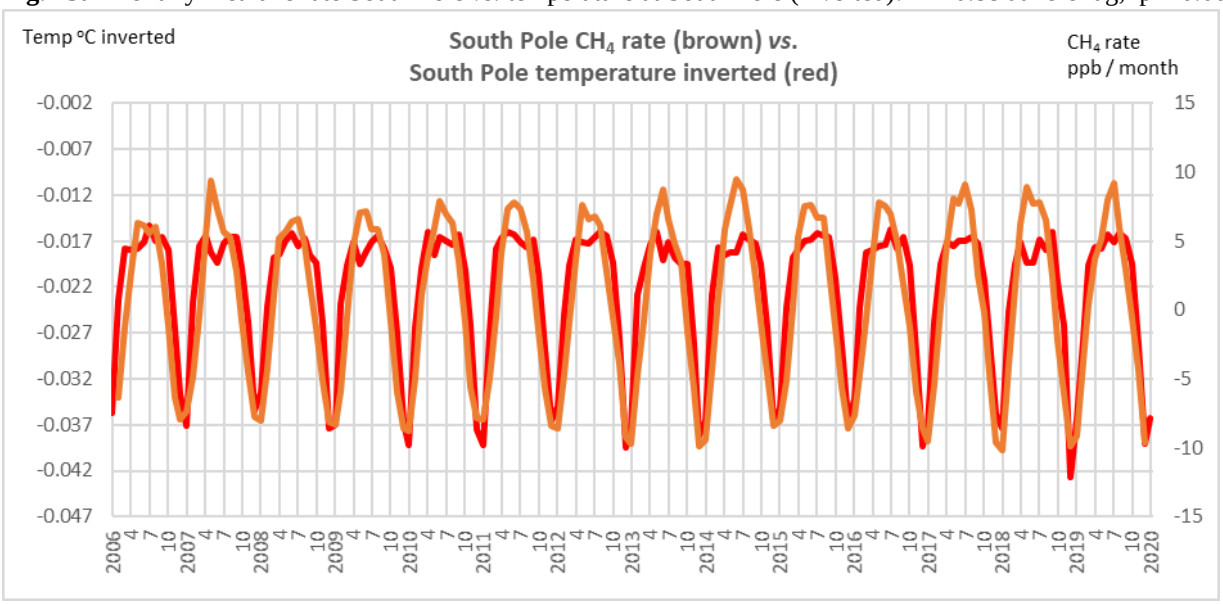

Fig. 13b Monthly South Pole methane rate *vs.* temperature at South Pole (inverted), using full continuous monthly methane record from February 1983

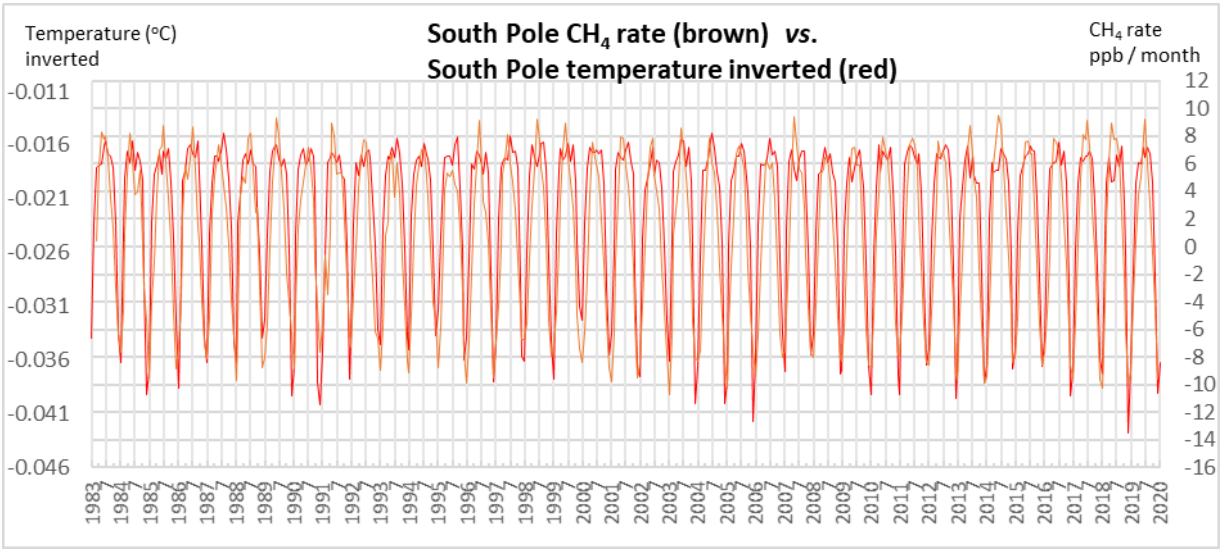

An example of the similarity of South Pole methane rate phenology to another Southern Hemisphere site, Cape Grim, is given in Fig. 14.

Fig. 14 Monthly methane rate South Pole *vs.* monthly methane rate Cape Grim (Tasmania)

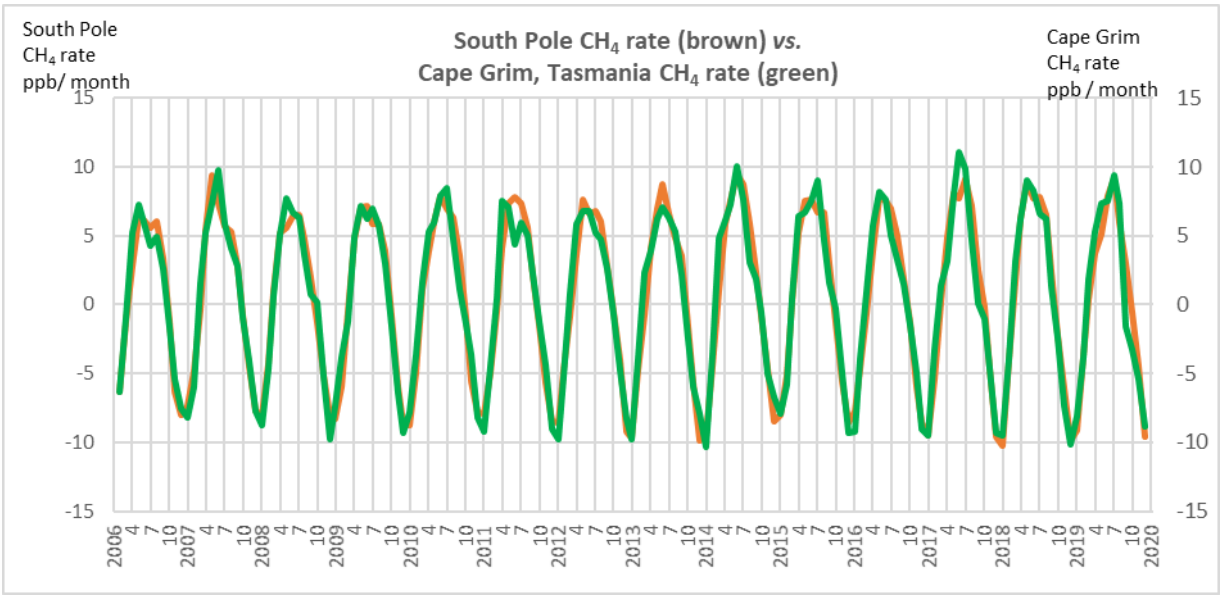

Time series for Antarctic sea ice rate, a local temperature and South Pole methane rate are given in Figs. 15 and 16.

Fig. 15 Monthly Antarctic sea ice extent rate *vs.* temperature at South Pole (inverted)

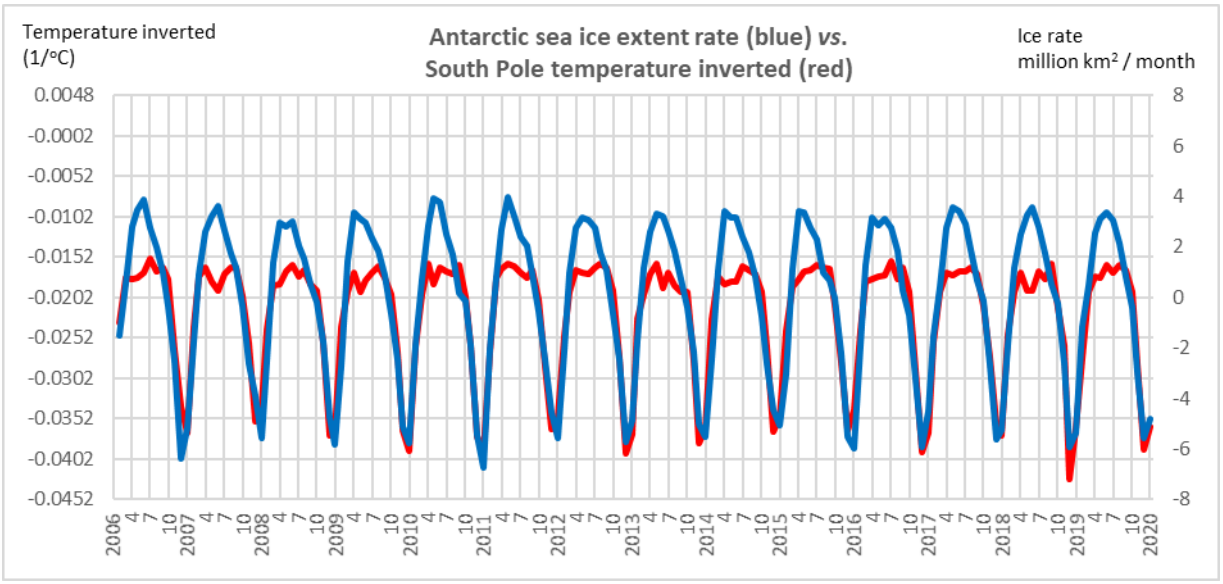

Fig. 16 Monthly Antarctic sea ice extent rate *vs.* monthly methane rate South Pole, 6 month moving average for both variables

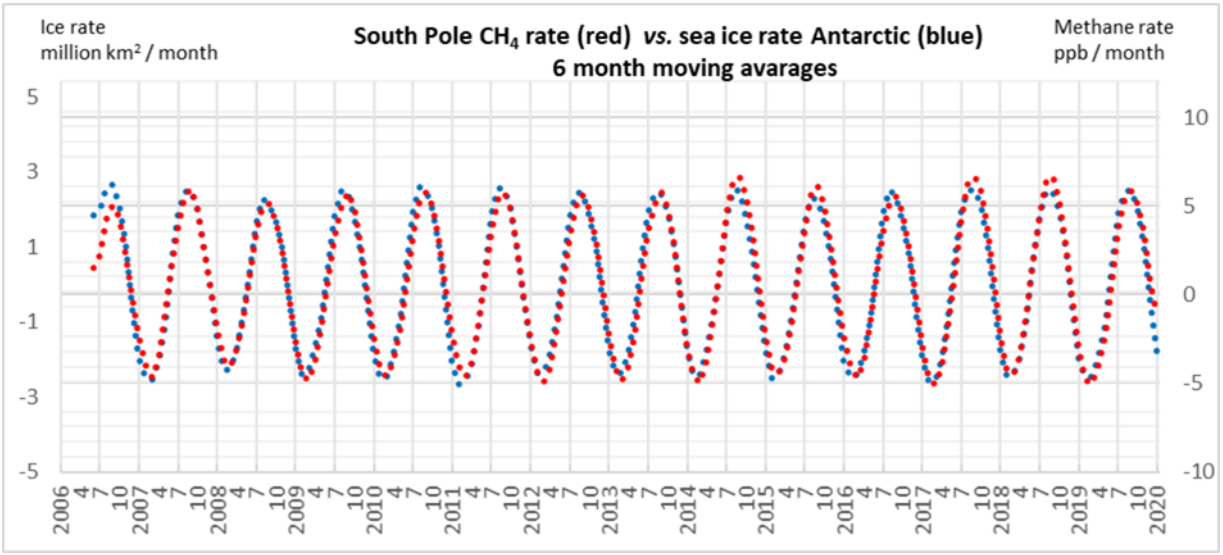

Discussion

Air temperature at or near the Poles peaks in very close synchrony with regional peaks in sea ice melt (Figs. 10 and 15). It will also be correlated with a range of other abiotic and biotic variables with various lags, such as Northern Hemisphere snow (Fig. 9). Air temperature at high latitude sites leads the global carbon dioxide rate with a greater lag of carbon dioxide behind the Antarctic than the Arctic temperature (Fig. 2 and Fig. 3).

The rates of change of globally representative levels of carbon dioxide and methane are very strongly correlated with the rate of change of global ('Arctic plus Antarctic') sea ice (Figs. 1 and 4). The rate of change of methane at Mauna Loa has similar phenology but greater amplitude (Fig. 5). At the South Pole, methane rates are very highly synchronous with Antarctic sea ice extent rates (Fig. 16), as are other regional methane rates (Hambler & Henderson 2020b). The lag of 5 - 7 months between the peak Antarctic temperature (and sea ice melt) and the fastest decline of

global methane and global carbon dioxide suggest a strong Antarctic influence on these gases (Fig. 1 and Fig. 4). It may take months for the effects of temperature on gas flux in the Antarctic to reach the Northern Hemisphere.

The extremely strong predictive power of global total sea ice for carbon dioxide and methane is notable - revealing possible causality or high predictive power for the actual cause. The two peaks in global sea ice rate result from the peak temperatures in the two Hemispheres. Global carbon dioxide and methane rates also have twin peaks which are similarly separated (Fig. 6). We propose that whatever dominates the fluxes of these gases makes strong contributions at high latitudes in both Hemispheres.

Temperature in at least one Artic recording site has a close synchrony with carbon dioxide (Fig. 7) and methane (Fig. 8) flux rates at the site (Alert, Canada). Other high-latitude Northern Hemisphere recording sites in the NOAA network have similar carbon dioxide and methane phenology to Alert (Hambler & Henderson, 2020a, b). Peak negative carbon dioxide flux (indicating drawdown or destruction of the gas) usually occurs synchronously with peak atmospheric temperature in the Artic summer (July, Fig. 7). This is also synchronous with peak decline in Arctic ice extent (Fig. 10). However, peak negative methane flux at Alert (Fig. 8) occurs about one month earlier than peak temperature and peak sea ice melt in the whole Arctic, which we suggest results from an influence of the biota or other abiotic factors on methane dynamics in the Arctic. Arctic sea ice as a whole can not be the dominant causal variable in this region at least, but there are regional differences in sea ice phenology, and Alert methane peak decline is more closely synchronous with the Barents Sea ice rate (Hambler & Henderson, unpublished). Peak rate of decline of Arctic methane is also closely synchronous with peak snow extent decline in the Northern Hemisphere, with Alert lagging snow melt by about a month (Fig. 9), consistent with putative terrestrial influences such as increased methanogenic microbial activity. Peak methane emission from Arctic mires can occur near peak summer air temperature (Jackowicz-Korczyński et al 2010).

Peak negative methane flux is synchronous with peak temperature at the South Pole (Fig. 13) but carbon dioxide rate at the South Pole lags one month behind the peak temperature which occurs December / January (Fig. 12). Similarly, methane rates slightly lead carbon dioxide rates globally and at Mauna Loa (Figs. 4 - 6). Intriguingly, South Pole temperature peaks simultaneously with peak rates of decline in both methane and carbon dioxide at the coastal and marine Antarctic sites in the NOAA network (Palmer, Syowa, Halley, Drake Passage) and is also simultaneous with peak Antarctic sea ice melt (Hambler & Henderson, 2020a, b). There may be differential transport, production or removal processes for methane and carbon dioxide after a synchronous monthly pattern is imprinted in the two gases at the edge of the Antarctic continent. High latitude sites in the Southern Hemisphere have very similar methane phenology (*e.g.* Fig. 14 and Hambler & Henderson 2020b) suggesting a very well-mixed southern air mass and / or a large-scale causal process.

The synchronous decline and rise in carbon dioxide and methane at many sites would most parsimoniously be explained by a single mechanism. These results are broadly consistent with our proposals that sea ice is either involved in the decline of atmospheric carbon dioxide and methane or is extremely strongly corelated with an unknown variable causing fluxes of the gases (Hambler & Henderson 2020a, b). We argue the extremely high correlations between sea ice and fluxes of both gases are more plausibly due to physical or chemical processes than to ecological ones (Hambler & Henderson 2020a, b). In particular, we suggest the peak negative gas rates may relate to ice melt and absorption by cold water undersaturated in these gases (Wiesenburg & Guinasso Jr 1979). The peak positive rates may relate to expulsion of gas during sea ice formation (degassing), marine emissions, and other physical and biological processes (Hambler & Henderson 2020a, b).

The conventional explanation of the terrestrial biota of the Northern Hemisphere driving the carbon dioxide seasonal cycle (Keeling et al 2001; Buermann et al 2007; Keeling 2008; IPCC 2013) does not explain the similar patterns of global carbon dioxide and methane which have many different biological and abiotic sources and sinks (IPCC 2013). A major factor implicated in removing atmospheric methane, the hydroxyl radical (OH) (Mastepanov et al 2008; Salby 2012; Ciais et al 2013) is created by photodissociation and thus would be expected to be temperature-dependent with latitudinal variation in amplitude. However, methane rate lags further behind peak temperature nearer the equator (Hambler & Henderson 2020b) suggesting net methane loss is not fastest where there is most sunlight. Moreover, to our knowledge there is no reported directly causal reason for OH to vary synchronously with carbon dioxide rate (as it often does regionally).

A lag of 7 months between temperature and carbon dioxide rate is consistent with the observed lag of about 9 - 10 months between temperature and carbon dioxide level (Humlum et al 2013; Salby 2013), suggesting South Pole air temperature is a very good proxy for a variable driving the annual carbon cycle. South Pole air temperature and Antarctic sea ice extent rate should both have predictive power for the 'global' carbon dioxide level 10 months in advance. Our results are consistent with a proposed sequence of events driving carbon dioxide changes starting in the Southern Hemisphere (Humlum et al 2013).

Inter-annual variation in monthly rates leads to net accumulation or loss of methane and carbon dioxide from the atmosphere. Both the amplitude and phase of methane rates in many sites in the Southern Hemisphere south of about 25ºS are very similar (Hambler & Henderson 2020b, and *e.g.* Fig. 14) suggesting large-scale common forcing. A variable such as temperature which correlates strongly with the amplitude of the annual cycle (*e.g.* Fig. 13) could help explain net global trends: for example, warm years generally have higher sea ice melt rates and more negative gas rates which might be partially caused by dissolution in melt water.

Conclusions

We suggest other variables be examined that might be influenced by temperature or insolation which might drive fluxes of carbon dioxide and methane. These include, for example, marine and terrestrial productivity and the hydroxyl radical (for methane). However, our correlations between sea ice rates and these greenhouse gases are the strongest with a putative cause that we are aware of - and we suggest they are a priority for further investigation and empirical tests of causality and mechanism. The global and Antarctic cycle of both gases have similarities suggesting the same processes or regions are involved in the dominant fluxes for both, despite their very different biological properties.

If temperature drives the annual cycle of carbon dioxide and methane then variation in temperature between years could cause changes in the annual rate of accumulation of these gases (Hambler & Henderson 2020a, b) and a common mechanism could cause the observed similarity of long term changes in these gases (Salby 2012, 2013). Given the high economic, social and environmental costs (Hambler & Canney 2013) of attempting to manipulate the flux of greenhouse gases it is paramount that natural fluxes be identified and partitioned to deduce the relative scale of human influence upon them.

Acknowledgements

We thank all sources listed in Table 1 or indicated in the metadata on the hosting websites.

Declarations

Funding None.

Conflict of interest / Competing interest The authors have no conflict of interest / competing interests.

Availability of data and material Data are available from the online providers indicated in Table 1. R code can be provided upon reasonable request.

Open Access

References

Buermann, W., Lintner, B.R., Koven, C.D., Angert, A., Pinzon, J.E., Tucker, C.J. & Fung, I.Y. (2007) The changing carbon cycle at Mauna Loa Observatory. *Proceedings of the National Academy of Sciences*, **104**, 4249-4254.

Bushinsky, S.M., Landschützer, P., Rödenbeck, C., Gray, A.R., Baker, D., Mazloff, M.R., Resplandy, L., Johnson, K.S. & Sarmiento, J.L. (2019) Reassessing Southern Ocean air sea CO_2 flux estimates with the addition of biogeochemical float observations. *Global Biogeochemical Cycles,* **33,** 1370-1388.

Ciais, P., Sabine, C., Bala, G., Bopp, L., Brovkin, V., Canadell, J., Chhabra, A., Defries, R., Galloway, J., Heimann, M., Jones, C., Le Quéré, C., Myneni, R.B., Piao, S & Thornton, P. (2013) Carbon and other biogeochemical cycles. In: *Climate change 2013: the physical science basis. Contribution of Working Group I to the Fifth Assessment Report of the Intergovernmental Panel on Climate Change* (ed. by T. Stocker, D. Qin, G.-K. Plattner, M. Tignor, S. Allen, J. Boschung, A. Nauels, Y. Xia, V. Bex & P. Midgley), pp. 465-570. Cambridge University Press, Cambridge, United Kingdom.

Dlugokencky, E.J., Mund, J.W., Crotwell, A.M., Crotwell, M.J. & Thoning, K.W. (2020a) Atmospheric carbon dioxide dry air mole fractions from the NOAA GML Carbon Cycle Cooperative Global Air Sampling Network, 1968-2019, Version: 2020-07. https://doi.org/10.15138/wkgj-f215. Accessed 1 August 2020.

Dlugokencky, E.J., Crotwell, A.M., Mund, J.W., Crotwell, M.J. & Thoning K.W. (2020b) Atmospheric methane dry air mole fractions from the NOAA GML Carbon Cycle Cooperative Global Air Sampling Network, 1983-2019, Version: 2020-07, https://doi.org/10.15138/VNCZ-M766. Accessed 1 August 2020.

Dlugokencky, E. (2021) Ed Dlugokencky, NOAA/GML (www.esrl.noaa.gov/gmd/ccgg/trends_ch4/). Accessed 1 January 2021.

Geilfus, N.-X., Pind, M., Else, B., Galley, R., Miller, L., Thomas, H., Gosselin, M., Rysgaard, S., Wang, F. & Papakyriakou, T. (2018) Spatial and temporal variability of seawater pCO_2 within the Canadian Arctic Archipelago and Baffin Bay during the summer and autumn 2011. *Continental Shelf Research,* **156,** 1-10.

Hambler, C. & Canney, S.M. (2013) *Conservation*. Cambridge University Press, Cambridge, United Kingdom.

Hambler, C. & Henderson, P.A. (2020a) Sea ice and carbon dioxide. Working Paper, version 2. https://ora.ox.ac.uk/objects/uuid:640a0c7e-6b55-4aff-a9cc-f47f6b490254

Hambler, C. & Henderson, P.A. (2020b) Sea ice and methane. Working paper, version 1. https://arxiv.org/pdf/2012.00839.

Henderson, P.A. (2021). *Ecological Methods*. Oxford University Press, Oxford, United Kingdom.

Humlum, O., Stordahl, K. & Solheim, J.-E. (2013) The phase relation between atmospheric carbon dioxide and global temperature. *Global and Planetary Change*, **100,** 51-69.

IPCC (2013) *Climate Change 2013: The physical science basis. Contribution of Working Group I to the Fifth*

Assessment Report of the Intergovernmental Panel on Climate Change (ed. by T. Stocker, D. Qin, G.-K. Plattner, M. Tignor, S. Allen, J. Boschung, A. Nauels, Y. Xia, V. Bex & P. Midgley), Cambridge University Press, Cambridge, United Kingdom.

Jackowicz-Korczyński, M., Christensen, T.R., Bäckstrand, K., Crill, P., Friborg, T., Mastepanov, M., & Ström, L. (2010) Annual cycle of methane emission from a subarctic peatland. *Journal of Geophysical Research Biogeosciences*, **115**, G02009.

Keeling, C., Piper, S., Bacastow, R., Wahlen, M., Whorf, T., Heimann, M. & Meijer, H. (2001) Exchanges of atmospheric CO_2 and $13CO_2$ with the terrestrial biosphere and oceans from 1978 to 2000. In: *Exchanges of atmospheric* CO_2 *and 13*CO_2 *with the terrestrial biosphere and oceans from 1978 to 2000. I. Global aspects, SIO Reference Series, No. 01-06*, pp. 1-88. Scripps Institution of Oceanography, San Diego.

Keeling, R.F. (2008) Recording Earth's vital signs. *Science*, **319,** 1771-1772.

Mastepanov, M., Sigsgaard, C., Dlugokencky, E.J., Houweling, S., Ström, L., Tamstorf, M.P. & Torben R. Christensen, T.R. (2008) Large tundra methane burst during onset of freezing. *Nature*, **456,** 628–630.

MOSAiC (2019) The key to the Arctic puzzle. From https://www.mosaic-expedition.org/science/arctic-climate/. Accessed 29 October 2019.

Resplandy, L., Keeling, R., Rödenbeck, C., Stephens, B., Khatiwala, S., Rodgers, K., Long, M., Bopp, L. & Tans, P. (2018) Revision of global carbon fluxes based on a reassessment of oceanic and riverine carbon transport. *Nature Geoscience*, **11,** 504-509.

Salby, M. (2012) *Physics of the atmosphere and climate*, 2nd edn. Cambridge University Press, Cambridge, United Kingdom.

Salby, M. (2013) Presentation Prof. Murry Salby in Hamburg on 18 April 2013. https://www.youtube.com/watch?v=2ROw_cDKwc0&feature=youtu.be. Accessed 9 February 2021.

Vancoppenolle, M. & Tedesco, L. (2017) Numerical models of sea ice biogeochemistry. In: *Sea ice*, 3rd edn. (ed. by D.N. Thomas), pp. 492-515. Wiley, New Jersey.

Wiesenburg, D.A. & Guinasso Jr, N.L. (1979) Equilibrium solubilities of methane, carbon monoxide, and hydrogen in water and sea water. *Journal of Chemical and Engineering Data*, **24,** 356-360.

Winkler, A.J., Myneni, R.B., Alexandrov, G.A. & Brovkin, V. (2019) Earth system models underestimate carbon fixation by plants in the high latitudes. *Nature Communications*, **10,** 1-8.